

Supporting Information for Numerical Modeling of Acousto-Plasmonic Coupling in Metallic Nanoparticles

Ophélie Saison-Francioso, Gaëtan Lévêque, and Abdellatif Akjouj

Institut d'Électronique, de Microélectronique et de Nanotechnologie, CNRS UMR 8520,
Département de Physique, FST, Université de Lille, 59655 Villeneuve d'Ascq, France

VALIDATION TESTS FOR ACOUSTIC SIMULATIONS

Table S1 shows finite element calculation for the breathing mode eigenfrequency of a free gold nanosphere of radius $r=30$ nm. Simulations have been performed on a quarter of sphere in order to reduce memory and computation time. Six different average mesh sizes have been tested in order to verify mesh independence of the results. Actually, we notice a difference of about 0.1% between the frequencies obtained for the largest and the finest meshes. Moreover, according to Lamb's model, the eigenfrequencies of the $l=0$ spheroidal vibration mode of a free isotropic sphere can be obtained by searching the roots of the following equation¹:

$$\frac{\tan\left(2\pi\nu\frac{r}{v_L}\right)}{2\pi\nu\frac{r}{v_L}} = \frac{1}{1 - \frac{(\pi\nu)^2 r^2}{v_T^2}} \quad (1)$$

where ν is the eigenfrequency, r is the sphere radius, v_L and v_T are the longitudinal and transverse speeds of sound. The numerical analysis of **equation 1** gives a breathing mode frequency of 50.6240 GHz for the considered sphere which is in agreement with the finite element calculations. The Lamé parameters describing gold elastic properties in FreeFem calculations are taken from reference 2 and used to determine the longitudinal and transverse speeds of sound ($v_L=3239.97$ m/s, $v_T=1200.17$ m/s).

Mesh size (nm)	Number of nodes	Frequency (GHz)	Relative error (%)
2.50	1777	50.6724	0.0956
2.00	3117	50.6545	0.0602
1.75	4421	50.6481	0.0476
1.50	6716	50.6412	0.0340
1.25	11009	50.6360	0.0237
1.00	20858	50.6316	0.0150

Table S1 : Finite element calculation of the breathing mode eigenfrequency of a free gold nanosphere of radius $r=30$ nm for different average mesh sizes and relative error compared to theory (**eq. 1**).

Figure S1 shows acoustic simulations results for the vibration modes of a free gold rod and a free gold prism. Different mesh sizes have been considered. In the article, the calculations for the rod have been performed with a mesh counting 8507 nodes. For the extension/contraction mode of the rod length, the mesh counting 893 nodes gives an evaluation of the eigenfrequency 0.2648 % higher compared to the article value and the mesh having 22319 nodes gives an eigenfrequency 0.0251 % smaller. For the breathing mode of the rod, the mesh having 893 nodes gives an evaluation of the eigenfrequency 0.3309 % higher compared to the article value and the mesh having 22319 nodes gives an eigenfrequency 0.0308 % smaller. Concerning the prism, calculations have been performed with a mesh counting 21667 nodes. The mesh having only 1804 nodes gives an evaluation of the eigenfrequency of the stretching/shrinking mode of the prism corners 0.0813 % higher compared to the article value and the mesh having 41890 nodes gives an eigenfrequency 0.0048 % smaller.

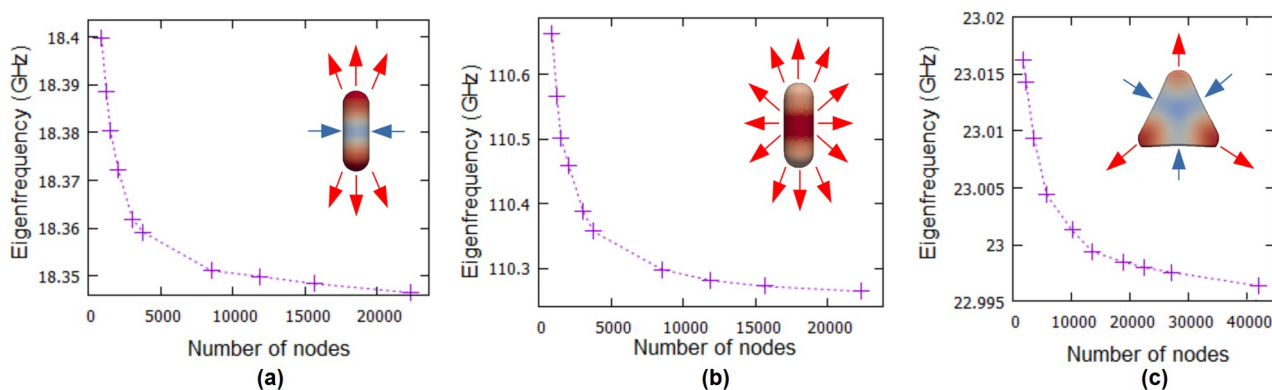


Figure S1 : Acoustic vibration modes eigenfrequencies of free gold nanoparticles calculated by FEM **(a)** Extension/contraction mode of the rod length (length=61 nm, width=22 nm) **(b)** Breathing mode of the rod (length=61 nm, width=22 nm) **(c)** Stretching/shrinking mode of the prism corners (thickness=25 nm, height=base=50 nm).

VALIDATION TESTS FOR OPTICAL SIMULATIONS

Figure S2 shows that finite element calculations agree well with Mie theory. Mie theory calculations have been performed using PyMieScatt, a Mie scattering package implemented in Python.³ Furthermore, simulations made for three different meshes confirm the mesh independence of the results. **Figure S3** points out the validity of the radial basis function interpolation method to transfer deformed geometries between acoustic and optical calculations. Concerning the evaluation of the resonance wavelength, the relative error between finite element calculation using RBFi and Mie theory calculation is about 0.02 %. **Figure S4** illustrates the mesh independence of our results through the examples of the rod and the prism which have a more complex shape than the sphere.

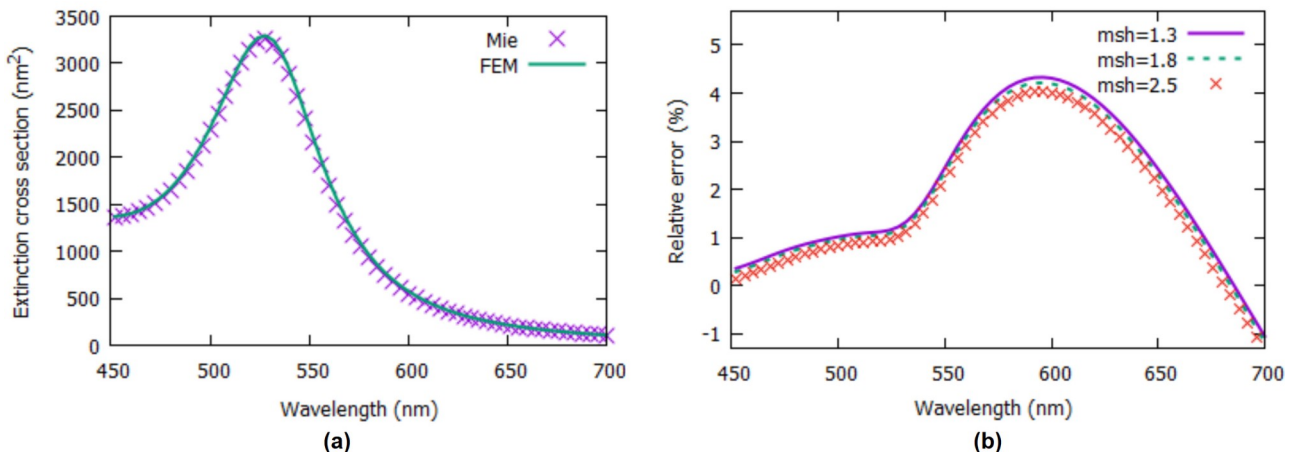


Figure S2 : (a) Extinction cross sections calculated by FEM and by Mie theory of a gold nanosphere of radius $r=30$ nm situated in a homogeneous dielectric host matrix ($RI=1.3$). (b) Relative error between finite element results and Mie theory for three different average mesh sizes ($msh=1.3, 1.8$ and 2.5 nm).

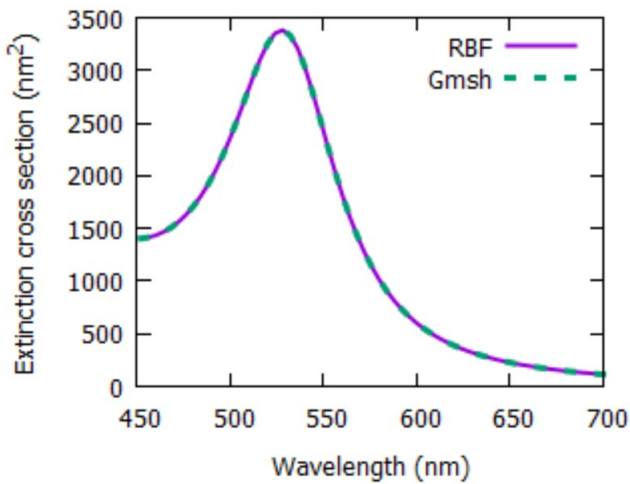


Figure S3 : Finite element calculation of the extinction cross sections of a gold nanosphere situated in a homogeneous dielectric host matrix ($RI=1.3$) which radius ($r=30$ nm) is increased by $\Delta r=+0.24$ nm, due to optomechanical coupling with the sphere breathing mode, without modification of the gold dielectric constant. The purple curve is obtained applying the RBFi method on a sphere with radius 30nm whose radius is increased the breathing mode. Green dashed curve is obtained by creating a mesh in a sphere with radius 30.24 nm directly with Gmsh.

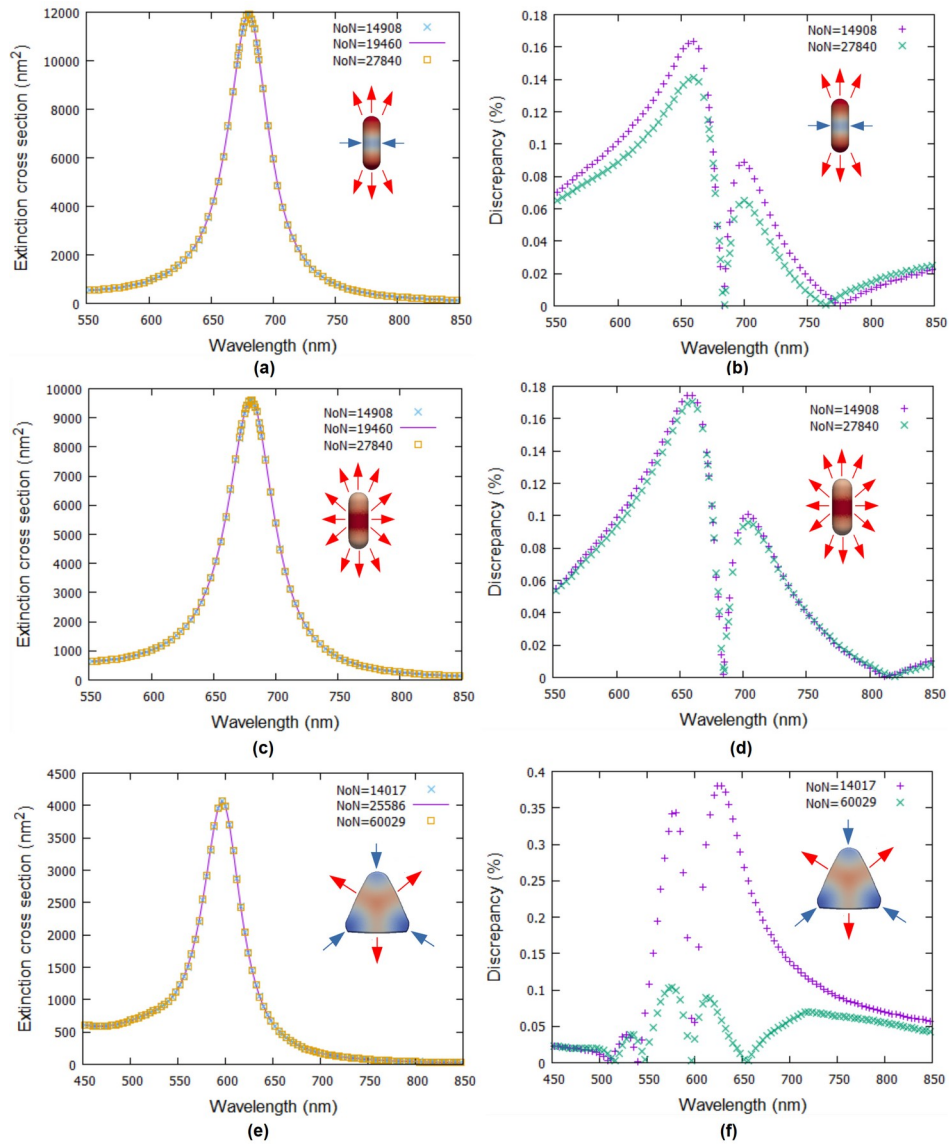


Figure S4: Optical spectra of the gold rod and prism in case of acousto-plasmonic coupling (Shape+ED+DP) for three different meshes characterized by their number of nodes (NoN). **(a)** Coupling with the extension/contraction mode of the rod length (length variation: $\Delta h = +1.2$ nm). **(c)** Coupling with the rod breathing mode (width variation: $\Delta w = +0.2$ nm). **(e)** Coupling with the stretching/shrinking mode of the prism corners (height variation: $\Delta h = -0.51$ nm). **(b)** **(d)** **(f)** Discrepancy between the NoN=19460 mesh for the rod and the NoN=25586 mesh for the prism, which correspond to the meshes used in the article, and the two other meshes.

REFERENCES

1. *Handbook of Nanophysics: Nanoparticles and Quantum Dots*; Sattler, K. D., CRC Press: Boca Raton, 2011.
2. Prost, A.; Poisson, F.; Bossy, E. Photoacoustic Generation by a Gold Nanosphere: From Linear to Nonlinear Thermoelastics in the Long-Pulse Illumination Regime. *Phys. Rev. B* **2015**, *92*, 115450.
3. Sumlin, B. Python Mie Scattering package. <https://pymiescatt.readthedocs.io/en/latest/> (accessed March 3, 2020).